J Mater Sci (2008) 43:3982–3988
DOI 10.1007/s10853-007-2235-0

INTERGRANULAR AND INTERPHASE BOUNDARIES IN MATERIALS

Study of InN/GaN interfaces using molecular dynamics

J. Kioseoglou · E. Kalessaki · G. P. Dimitrakopulos · Ph. Komninou · Th. Karakostas

Received: 6 July 2007 / Accepted: 17 October 2007 / Published online: 21 March 2008
© Springer Science+Business Media, LLC 2008

Abstract Epitaxial growth of thin films is, in general, based on specific interfacial structures defined by a minimum of interfacial energy and usually influenced by the structural mismatch. In the present study, the structures and energies of (0001) InN/GaN epitaxial interfaces are studied using the Tersoff interatomic potential. The potential describes the metallic and intermetallic interactions sufficiently well and is assembled in order to accurately reproduce the lattice and elastic parameters of wurtzite Ga(In)-Nitrides. Different configurations are examined for each interface depending on polarity and atomic stacking. It is shown that the interfacial structures of InN thin films grown with indium polarity interfaces exhibit lower self-energies than those of N-polarity. Although the substrate and the epilayer were assumed to exhibit the wurtzite crystal structure, both wurtzite and zinc-blende type atomic stackings are possible at the interfacial region since they were found energetically degenerate within the accuracy of our model. Finally, the spatial location of the epitaxial interface is also energetically defined. Epitaxial interfaces in this system can in principle be imagined to pass through so-called single or double atomic bonds, but the former case was energetically more favourable.

J. Kioseoglou · E. Kalessaki · G. P. Dimitrakopulos · Ph. Komninou · Th. Karakostas (✉)
Department of Physics, Aristotle University of Thessaloniki, Thessaloniki 54124, Greece
e-mail: karakost@auth.gr

Introduction

During the last few decades it has become widely recognized that group III nitrides differ to a significant extent from traditional III–V semiconductors. This difference is mostly attributed to two important features. First, due to nitrogen's large electronegativity the chemical bonds in nitrides are characterized by high ionicity in comparison to phosphides, arsenides and antimonides. Second, a much higher mismatch between the atomic radii of cations and anions exists in the case of nitrides [1, 2].

Epitaxial growth of heterostructures results in many semiconductor-based opto and micro-electronic devices. An important factor determining the quality of the aforementioned heterostructures is the atomic scale structure of the interfaces. So far the interfacial structures of (0001) GaN/ZnO [3], GaN/AlN [4] and GaN/ZrB_2 [5] have been studied using ab initio methods. However, such studies can employ relatively small numbers of atoms and thus cannot take fully into account the relaxation of the lattice mismatch by geometrically necessary defects.

On the subject of preferable polarity for the InN/GaN heterostructures several studies have been performed during the last few years since polarity strongly affects material properties. According to Refs. [6, 7], InN epilayers follow the polarity of the GaN template. The study of Dimakis et al. [8] shows that InN growth on Ga-face GaN (0001) by RFMBE results in In-face InN following a two-step growth process. Due to the nitridation step often employed when GaN is grown on sapphire, the template may exhibit N polarity [7]. Moreover, different polarity materials also result by different growth conditions as can be seen in the cases of GaN layers grown on sapphire [9, 10]. Ga polarity layers are grown under high nitridation temperature while low nitridation temperature results in

N-polarity materials [9]. Equivalent impact with the nitridation temperature is found for the growth temperature but it is also stated that the use of an AlN buffer layer under low-growth temperatures results in Ga face polarity materials [10]. A recent study [11] states that InN grown by MOVPE on sapphire substrate usually exhibits In polarity while InN grown by MBE is usually N-polarity material.

The present paper investigates the structures and energies of the (0001) InN/GaN interfaces where a 10.9% lattice mismatch between the crystal lattices is involved. Different configurations were examined for each interface depending on polarity (III- or N-polarity) and interfacial structure (wurtzite or zinc blende stacking). To sufficiently account for this misfit a total of ~15,000 atoms and the Tersoff interatomic potential were used for the energetic calculations. Our potential sufficiently describes the metallic and intermetallic interactions and was assembled in order to accurately reproduce the lattice and elastic parameters of wurtzite Ga(In)-Nitrides [12]. Stable relaxed interfacial structures and energies were obtained for all the configurations studied. In section "Computational method" the applied computational method is analytically presented. In section "Results and discussion" the results are given and in section "Conclusions" the conclusions are presented.

Computational method

In the present study we used the bond-order Tersoff potential [12–17], where the total potential energy is given by

$$E = \frac{1}{2}\sum_{j \neq i} V_{ij}, \quad (1)$$

where V_{ij} is the bond energy between atoms i and j

$$V_{ij} = f(r_{ij})[V_R(r_{ij}) - b_{ij}V_A(r_{ij})], \quad (2)$$

and r_{ij} is the interatomic distance.

The pair like attractive and repulsive energies are given as Morse-like terms

$$V_R(r_{ij}) = \left[\frac{Do}{S-1}\right]\exp\left[-\beta\sqrt{2S}(r_{ij} - r_o)\right], \quad (3)$$

$$V_A(r_{ij}) = \left[\frac{SDo}{S-1}\right]\exp\left[-\beta\sqrt{\frac{2}{S}}(r_{ij} - r_o)\right]. \quad (4)$$

The interaction is restricted in a sphere by a cut-off function

$$f(r_{ij}) = \begin{cases} 1 & r_{ij} < R - D \\ \frac{1}{2}\{1 - \sin[\pi(r_{ij} - R)/(2D)]\} & |r_{ij} - R| \le D, \\ 0 & r_{ij} > R + D \end{cases} \quad (5)$$

where R is the cut-off range and $2 \times D$ is the width of the region in which the function $f(r_{ij})$ changes smoothly from 1 to 0. The many-body term includes the angular dependency b_{ij} and the angular function $g_{ik}(\theta_{ijk})$ as described in detail elsewhere [12–16].

This potential was tuned in order to reproduce accurately the equilibrium lattice constant a, the axial ratio c/a, the internal parameter u, the binding energy, the formation enthalpy, the elastic constants and In-In interaction as described in detail elsewhere [12]. In particular, for Ga–N, Ga–Ga and N–N interactions the parameters given by Nord et al. [16] were used. For In–N interactions the parameters are modified slightly relative to those of the zinc blende structure [18] in order to describe the wurtzite structure. For In–In the parameters were determined by tailoring the sets of Nordlund et al. [18] for metallic In–In interaction (In *fct* lattice, Space Group: *I4/mmm*) [12]. For the intermetallic interactions (i.e. In–Ga) the parameterization of Ref. [18] was used.

For the construction of the bicrystals, InN and GaN supercells were created in the form of rectangular parallelepiped volumes by using the optimized lattice constants obtained from the interatomic potential. Each supercell comprised 21 MLs along [0001]. The exact dimensions of each supercell volume were $10 \times a$ along $[1\bar{2}10]$, $10 \times c$ along [0001] and $10 \times a \times 3^{1/2}$ along $[10\bar{1}0]$ (where a and c are the equilibrium lattice parameters). These InN and GaN bicrystal components, comprising a total of ~15,000 atoms, were then employed in order to construct all possible interfaces. The epilayer thickness was taken greater than the critical thickness for coherency strain relaxation. The interfaces were assumed to be initially abrupt and without any interdiffusion of atomic species. Periodic boundary conditions were applied along the basal plane (i.e. $[1\bar{2}10]$ and $[10\bar{1}0]$), while fixed boundaries were imposed along [0001]. The fixed boundary conditions were applied using the following methodology [19]: For Ga-polarity along the [0001] for InN and $[000\bar{1}]$ for GaN (or vice-versa for N-polarity) the supercells were divided into three zones defining a thin external zone (zone 1), a thin intermediate zone (zone 2) and the internal area (zone 3). This configuration is illustrated schematically in Fig. 1. The InN/GaN interface was constructed by combining zone 3 of InN with the equivalent zone of GaN. The thickness of zone 1 was greater than the maximum range of the potential, and the atoms were at fixed positions there. Zone 2 starts at the end of zone 1 and also extends further than the maximum range of the potential and up to zone 3. In zone 2 the atoms were relaxed but were not taken into account in energetic calculations. The energetic calculations were performed taking into consideration only the energies of the relaxed atoms in zone 3.

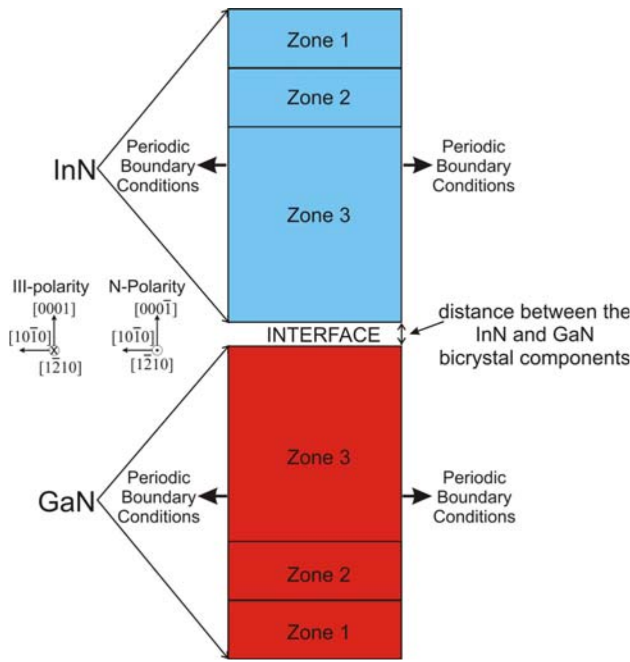

Fig. 1 The employed supercell configuration showing division into three zones defining a thin external zone (zone 1), a thin intermediate zone (zone 2) and the internal area (zone 3). The InN/GaN interface is constructed by combining the zone 3 of InN with the equivalent zone of GaN

The distance between the InN and GaN bicrystal components at the interfaces was optimized by use of the adaptive conjugate gradient fast relaxation procedure [20]. The minimum energy configurations were further relaxed from the temperature of 600 K slowly down to 0 K by a quasidynamic minimization procedure [21].

In our study, the obtained excess interfacial energies are independent of the growth conditions as explained in the following. As known, the interaction of an open system with its environment depends on the chemical potentials of its components. For the growth of undoped bulk solid III–N:

$$\mu^s_{\text{III-N}} = \mu_{\text{III}} + \mu_{\text{N}}, \tag{6}$$

where $\mu^s_{\text{III-N}}$ is the chemical potential for wurtzite III–N and μ_{III} and μ_{N} are the chemical potentials of III-type and nitrogen atoms, respectively. The heat of formation ΔH^f_{IIIN} is defined by:

$$\Delta H^f_{\text{III-N}} = \mu^s_{\text{III-N}} - \mu^s_{\text{III}} - \mu^g_{\text{N}_2}, \tag{7}$$

where μ^s_{III} and $\mu^g_{\text{N}_2}$ are the chemical potentials for solid III and gaseous nitrogen (N_2), respectively.

By taking into account that

$$\mu_{\text{III}} < \mu^s_{\text{III}}, \tag{8}$$

and

$$\mu_{\text{N}} < \mu^g_{\text{N}_2}, \tag{9}$$

we obtain the upper and lower limits for each potential:

$$\mu^s_{\text{III}} + \Delta H^f_{\text{III-N}} < \mu_{\text{III}} < \mu^s_{\text{III}}, \tag{10}$$

and

$$\mu^g_{\text{N}_2} + \Delta H^f_{\text{III-N}} < \mu_{\text{N}} < \mu^g_{\text{N}_2}. \tag{11}$$

By the use of a parameter λ ($0 \le \lambda \le 1$) we assume:

$$\mu_{\text{III}} = \mu^s_{\text{III}} + (1-\lambda)\Delta H^f_{\text{III-N}}, \tag{12}$$

and

$$\mu_N = \mu^g_{\text{N}_2} + \lambda \Delta H^f_{\text{InN}}, \tag{13}$$

where N-rich conditions are represented for $\lambda = 0$ and III-rich conditions for $\lambda = 1$.

If

$$\begin{aligned}\Delta\mu &= (\mu_{\text{III}} - \mu^s_{\text{III}}) - (\mu_{\text{N}} - \mu^g_{\text{N}_2}) \\ &= (\mu_{\text{III}} - \mu_{\text{N}}) - (\mu^s_{\text{III}} - \mu^g_{\text{N}_2}),\end{aligned} \tag{14}$$

and

$$\Delta\mu = (1-2\lambda)\Delta H^f_{\text{III-N}}, \tag{15}$$

then $\Delta\mu$ is restricted in the range

$$-\Delta H^f_{\text{IIIN}} \le \Delta\mu \le \Delta H^f_{\text{IIIN}}. \tag{16}$$

Let Ω_{D} be the total excess energy of a supercell that corresponds to the difference between the total energy E_{D} found by our interatomic potential calculations and the energy of a bicrystal supercell containing the same number of atoms. This energy corresponds to the excess energy of an interface at zero temperature and it is given by:

$$\begin{aligned}\Omega_{\text{D}}(\mu_{\text{III}}, \mu_{\text{N}}, \Delta\mu) = E_{\text{D}} &- \frac{1}{2}(n_{\text{In}} + n_{\text{N(for InN)}})\mu^s_{\text{InN}} \\ &- \frac{1}{2}(n_{\text{In}} - n_{\text{N(for InN)}})(\mu^s_{\text{In}} - \mu^g_{\text{N}_2}) \\ &- \frac{1}{2}(n_{\text{In}} - n_{\text{N(for InN)}})\Delta\mu \\ &- \frac{1}{2}(n_{\text{Ga}} + n_{\text{N(for GaN)}})\mu^s_{\text{GaN}} \\ &- \frac{1}{2}(n_{\text{Ga}} - n_{\text{N(for GaN)}})(\mu^s_{\text{Ga}} - \mu^g_{\text{N}_2}) \\ &- \frac{1}{2}(n_{\text{Ga}} - n_{\text{N(for GaN)}})\Delta\mu\end{aligned} \tag{17}$$

where n_{In}, n_{Ga} and n_{N} are the numbers of In, Ga and N atoms, respectively [22].

It should be noted that, following Eq. 17, the total excess energy depends on $\Delta\mu$ and thus on λ. Consequently the calculated energetic results depend on the growth conditions through λ (for $\lambda = 1$ (III -rich) $\Delta\mu = -\Delta H^{f}_{\mathrm{IIIN}}$ and for $\lambda = 0$ (N-rich) $\Delta\mu = \Delta H^{f}_{\mathrm{IIIN}}$). In our study, we maintained for all cases, $n_{\mathrm{In}} = n_{\mathrm{N\ (for\ InN)}}$ and $n_{\mathrm{Ga}} = n_{\mathrm{N\ (for\ GaN)}}$. Therefore,

$$\Omega_{\mathrm{D}}(\mu_{\mathrm{III}}, \mu_{\mathrm{N}}) = E_{\mathrm{D}} - \frac{1}{2}(n_{\mathrm{In}} + n_{\mathrm{N(for\,InN)}})\mu^{s}_{\mathrm{InN}} - \frac{1}{2}(n_{\mathrm{Ga}} + n_{\mathrm{N(for\,GaN)}})\mu^{s}_{\mathrm{GaN}}, \quad (18)$$

i.e. the excess energy of an interface in this work is indeed independent of the growth conditions. This is important for isolating the structural and chemical contribution to the interfacial energy. The interfacial energy per unit area, E_{int}, is given by:

$$E_{\mathrm{int}} = \frac{\Omega_{\mathrm{D}}}{A}, \quad (19)$$

where A is the interface area of the supercell $(10 \times a) \times (10 \times a\, 3^{1/2})$.

Results and discussion

The above-described methodology was applied to supercells that were constructed for all the possible atomic stackings at the interface (apart from those involving a polarity reversal at the interface). In particular, the following geometrical conditions were taken into account: (a) polarity, (b) atomic stacking and (c) location of the interface. With respect to (a), it is well known that the c axis in wurtzite III–N is polar. Thus, due to the fact that the [0001] direction is parallel to the III–N bond, conventionally, the structure has III polarity or N polarity depending on whether the III–N bonds point upwards or downwards, respectively.

With respect to atomic stacking, although in the present study only the wurtzite structure was considered for bulk InN and GaN, both wurtzite and zinc blende stackings were examined across the interfaces (i.e. ABABA and ABABCA stackings, respectively). These geometrical conditions are illustrated schematically in Fig. 2. It is proposed in literature that the zinc blende stacking may be favoured under certain conditions at the interface between epitaxially grown wurtzite layers [23]. This is confirmed by us as can be seen in the High Resolution Transmission Electron Microscopy (HRTEM) image of Fig. 3, that depicts an InN/GaN interface. (Experimental details for the growth conditions of the specimen and the conditions of the HRTEM experimental observations are presented elsewhere [24].) In Fig. 3 the stacking sequence along the [0001] axis is transformed locally from hexagonal wurtzite to cubic zinc blende.

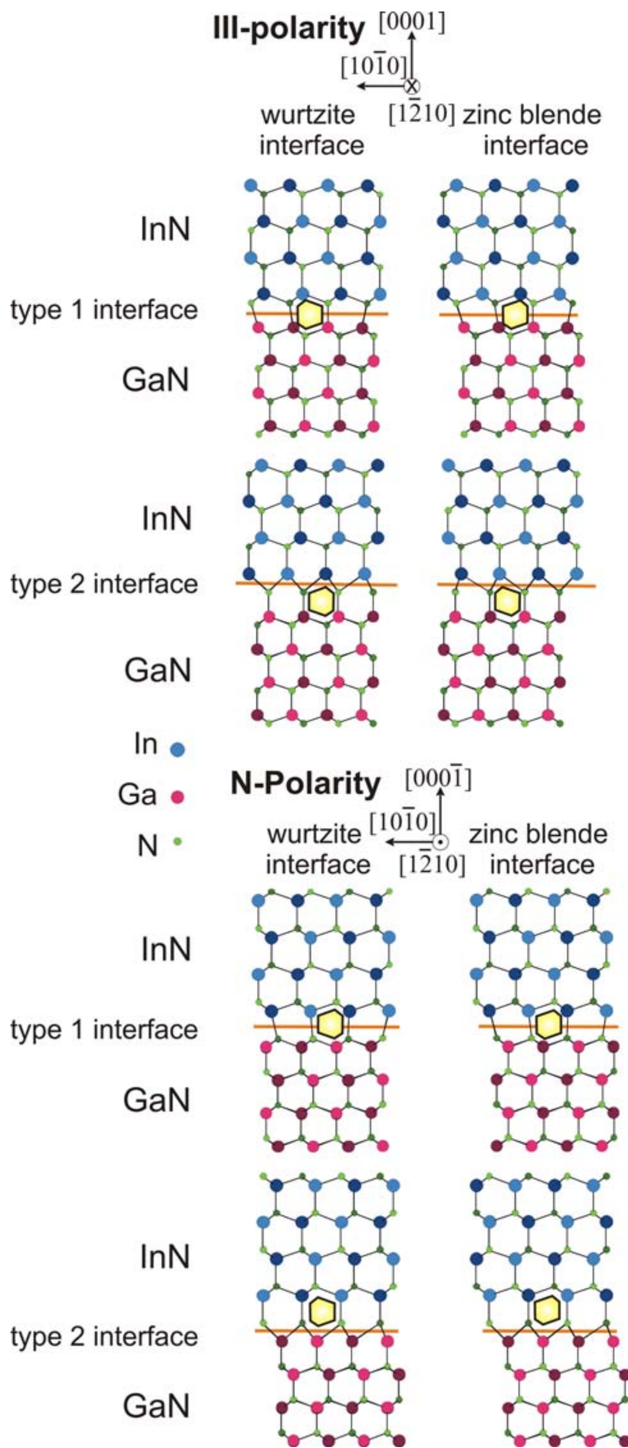

Fig. 2 The possible atomic stackings at the interface. Initial InN/GaN type 1 (cutting single bonds) and type 2 (cutting double bonds) interfaces for wurtzite and zinc blende interfacial structures viewed along [1$\bar{2}$10]. The wurtzite and zinc blende structural units are marked in yellow. The interface plane is indicated by lines, large and small circles denote III (Ga, In) and N atoms, respectively, coloured (grey) circles are at 0 level, and dark circles are at level $a/2$ along the projection direction

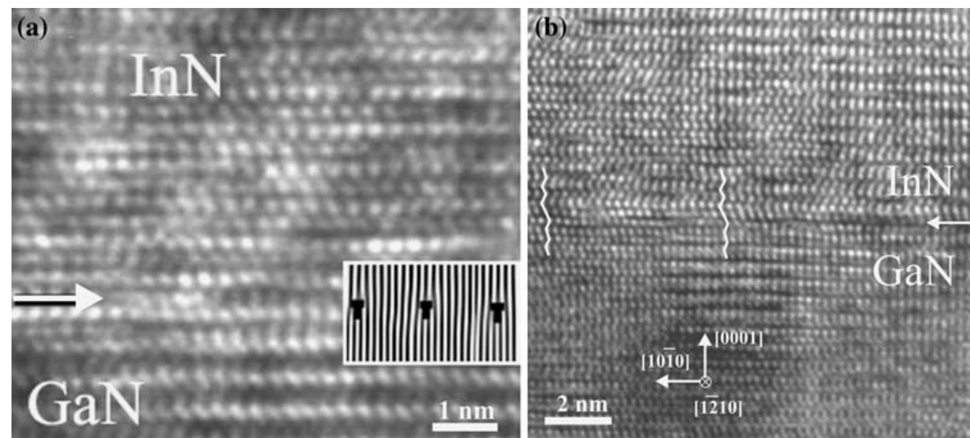

Fig. 3 (**a**) HRTEM images of the InN/GaN interface viewed along [1$\bar{2}$10] zone axis. FFT image (inset) using the in-plane spatial frequencies reveals the locations of the edge component of misfit dislocations as terminating {10$\bar{1}$0} GaN lattice fringes. (**b**) A change of the wurtzite stacking sequence along the InN/GaN interface is evidenced for the transformation of the interfacial structure from wurtzite to zinc blende (white spots represent the atomic columns)

Table 1 The interfacial energy per unit area for the type 1 and type 2 interfaces (i.e. cutting single or double bonds) having as reference zero level the calculated formation energy of the favourable InN/GaN interface (type 1, III-polarity, $E_{\text{int}} = 0.21$ eV/Å^2)

Interfacial stacking & material polarity	$\Delta E_{\text{int}}(\text{eV})/\text{Å}^2$
Type 1 interfaces	
Wurtzite stacking—III polarity	0
Wurtzite stacking—N polarity	+0.051
Zinc blende stacking—III polarity	0
Zinc blende stacking—N polarity	+0.059
Type 2 interfaces	
Wurtzite stacking—III polarity	+0.32
Wurtzite stacking—N polarity	+0.46
Zinc blende stacking—III polarity	+0.32
Zinc blende stacking—N polarity	+0.46

Finally the aforementioned (c) condition refers to the two possible locations that the interfacial plane can reside at, i.e. cutting either single or double bonds; the former is designated as type 1 plane and the latter as type 2. This leads overall to eight possible starting configurations to be relaxed as illustrated in Fig. 2.

In Table 1, the relative interfacial energies per unit area for the type 1 and type 2 interfaces are presented having as reference the formation energy of the energetically favourable InN/GaN interface (type 1, III-polarity, $E_{\text{int}} = 0.21$ eV/Å^2). It is shown that, in the type 1/III-polarity case, both the wurtzite and the zinc blende atomic stackings are favoured and the two stackings cannot be distinguished energetically under the present methodology. However this is in agreement with our experimental observations whereby both stackings are observed at the interfacial region (Fig. 3). Next favoured interfaces are the type 1/N-polarity ones. Again both the wurtzite and zinc blende stackings are energetically equivalent within the error interval of the interatomic potential calculations (0.01 eV/Å^2). On the other hand the type 2 interfaces generally exhibit higher energies.

In Fig. 4 the relaxed InN/GaN type 1 interfaces are illustrated in cross section viewed along ⟨1$\bar{2}$10⟩. The

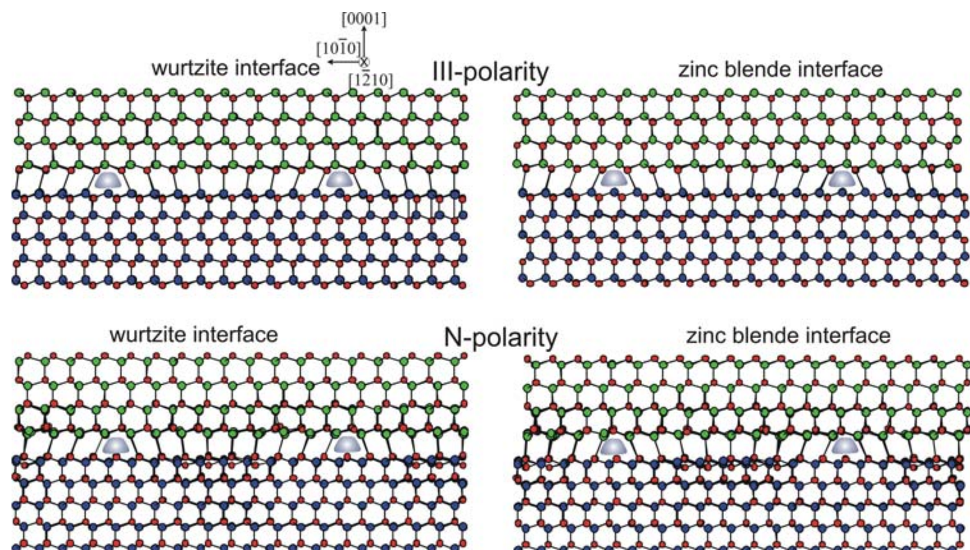

Fig. 4 Relaxed InN/GaN type 1 (cutting single bonds) interfaces for wurtzite and zinc blende interfacial structures viewed along [1$\bar{2}$10]. (Symbols are as in Fig. 2)

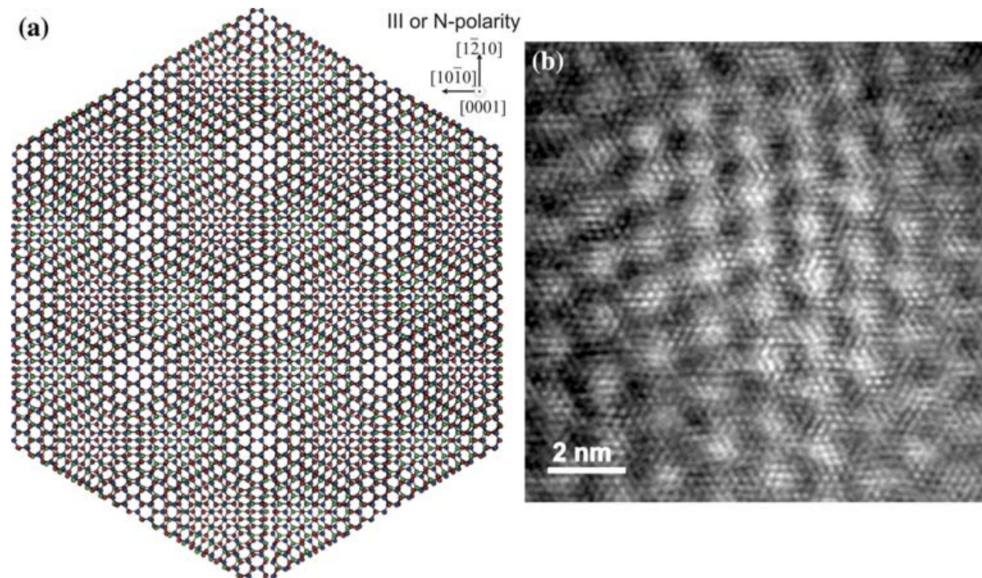

Fig. 5 (**a**) [0001] projection of the relaxed InN/GaN type 1 (cutting single bonds) interface having wurtzite interfacial structure. The two polarities are non-distinguishable when viewed along [0001]. (**b**) HRTEM image along the [0001] direction of InN/GaN interface. The moiré pattern reveals the regions of "good" and "bad" fit

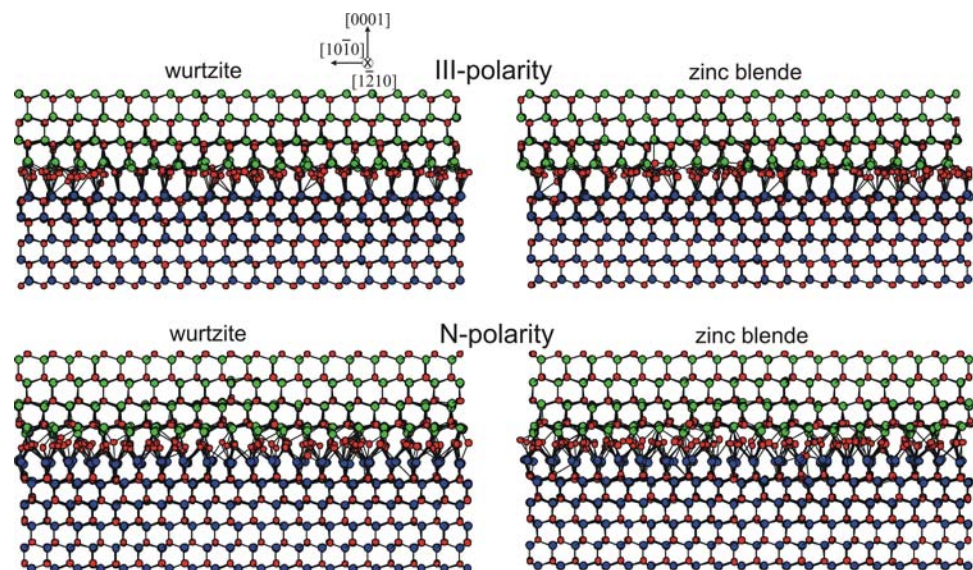

Fig. 6 Relaxed InN/GaN type 2 (cutting double bonds) interfaces for both polarities and for wurtzite and zinc blende interfacial structures. ($\langle 1\bar{2}10\rangle$ projection, symbols are as in Fig. 2)

atomic relaxed configuration along the N-polar interfaces is found to be quite different from the corresponding III-polar cases.

In Fig. 5a the [0001] projection of the wurtzite type 1 interface (Fig. 4a) is shown, while in Fig. 5b a plan-view HRTEM experimental micrograph along [0001] is given. In Fig. 5b moiré fringes that reveal the hexagonal symmetry of the (0001) interface are observed, and the "good" and "bad" fit regions are in good agreement with the relaxed structure of Fig. 5a.

In Fig. 6 the relaxed InN/GaN type 2 interfaces viewed along the $\langle 1\bar{2}10\rangle$ direction are presented. It is evident that the relaxed atomic configurations of the type 2 interfaces are very distorted in comparison to those of type 1 and consequently these interfaces exhibit much higher energies.

In Figs. 4 and 6, extra half planes can be identified in the projections along $\langle 1\bar{2}10\rangle$ corresponding to geometrically necessary misfit dislocations. In all cases the topological property of the misfit dislocations, the Burgers vector, is the same, i.e. $1/3\langle 1\bar{2}10\rangle$ as can be verified by circuit mapping.

Conclusions

The structures and energies of all possible InN/GaN interfaces have been studied by the use of interatomic potential calculations. Eight different possible cases were examined depending on polarity (III or N polarity), interfacial stacking (wurtzite or zinc blende type) and interfacial plane (cutting single or double bonds).

A detailed procedure was presented for the construction, relaxation and energetic investigation of the interface atomic configurations. It was evidenced that the III-polarity interfaces are energetically favourable compared to those of N-polarity. It is also concluded that the type 1 interfaces (cutting single bonds) are energetically favourable with respect to the type 2 interfaces (cutting double bonds). Wurtzite and zinc blende stackings along the interface are found energetically degenerate in the present study. The energy difference between the two interfacial phases is found smaller than the accuracy of our interatomic potential calculations and consequently they are not distinguishable. Both the wurtzite and zinc blende stackings were observed at the InN/GaN interface by HRTEM.

Further investigations by electronic structure calculations could be useful for distinguishing between wurtzite and zinc blende interfacial stackings since they reach a higher level of accuracy and could also be able to investigate the effect of lattice strain on the structural and electronic properties of the InN/GaN system.

Acknowledgement This work was supported by the EC under the contract MRTN-CT-2004-005583 (PARSEM).

References

1. Pankove JI, Moustakas TD (1998) In: Semiconductors and semimetals. Academic Press, New York
2. Morkoç H (2007) In: Nitride semiconductors and devices. Springer Series in Materials Science
3. Von Pezold J, Bristowe PD (2005) J Mater Sci 40:3051
4. Bernardini F, Fiorentini V (1998) Phys Rev B 57:R9427
5. Liu PL, Chizmeshy AVG, Kouvelakis J, Tsong IST (2005) Phys Rev B 72:245335
6. Mitate T, Mizuko S, Takahata H, Kakegawa R (2005) Appl Phys Lett 86:134103
7. Wang X, Yoshikawa A (2004) Prog Cryst Growth 48/49:42
8. Dimakis E, Tsagaraki K, Iliopoulos E, Komninou Ph, Delimitis A, Georgakilas A (2005) J Cryst Growth 278:367
9. Georgakilas A, Mikroulis S, Cimalla V, Zervos M, Kostopoulos A, Komninou Ph, Kehagias Th, Karakostas Th (2001) Phys Status Solidi (a) 188:567
10. Mikroulis S, Georgakilas A, Kostopoulos A, Cimalla V, Dimakis E, Komninou Ph (2002) Appl Phys Lett 80:2886
11. Nari H, Matsuka F, Araki T, Suzuki A, Manishi Y (2004) J Cryst Growth 269:155
12. Kioseoglou J, Komninou Ph, Karakostas Th (unpublished work)
13. Tersoff J (1989) Phys Rev B 39:5566
14. Tersoff J (1990) Phys Rev B 41:3248
15. Albe K, Nordlund K, Nord J, Kuronen A (2002) Phys Rev B 66:035205
16. Nord J, Albe K, Erhart P, Nordlund K (2003) J Phys: Condens Mat 15:5649
17. Benkabou F, Certier M, Aourag H (2003) Mol Simulat 29:201
18. Nordlund K, Nord J, Frantz J, Keinonen J (2000) Comp Mater Sci 18:283
19. Kioseoglou J, Dimitrakopulos GP, Komninou Ph, Polatoglou HM, Serra A, Bere A, Nouet G, Karakostas Th (2004) Phys Rev B 70:115331
20. Nordlund K (2007) In: Introduction to atomistic simulations 2006 Lecture notes, http://www.beam.acclab.helsinki.fi/~akuronen/atomistiset/lecturenotes/ as on 3 July 2007
21. Beeler JR, Kulcinski GL (1972) Agenda discussion: computer techniques in interatomic potentials and simulation of lattice defects. Plenum, New York, p 735
22. Qian GX, Martin R, Chadi D (1988) Phys Rev B 38:7649
23. Bourret A, Adelmann C, Daudin B, Rouviere J-L, Feuillet G, Mula G (2001) Phys Rev B 63:245307
24. Delimitis A, Komninou Ph, Dimitrakopulos GP, Kehagias Th, Kioseoglou J, Karakostas Th, Nouet G (2007) Appl Phys Lett 90:061920